USER GUIDE

PROMCOR : The full computation of Hydrogen lines in a spherically symmetric and optically thin medium, such as the solar corona

Martine Chane-Yook

martine.chane-yook@ias.u-psud.fr

Reviewed by:

Jean-Claude Vial
Jacques Dubau

Web access:

https://idoc.ias.u-psud.fr/MEDOC/Radiative transfer codes

Contents

1 Introduction

The PROMCOR code is inherited from PROM5 code and treats models where the thermodynamic parameters only depend on the distance from the Sun center. It is valid only for (coronal) media optically thin in all lines and continua. PROMCOR describes Non-LTE (NLTE) radiative transfer (1D) for hydrogen atom using partial frequency redistribution for resonance lines of hydrogen. We solve the equations of radiative transfer (here limited to a simple integration), statistical equilibrium of level populations, and ionization equilibrium for the hydrogen atom using an iterative method.

For a given model of atmosphere defined by temperature, T, pressure, P, microturbulent velocity, V, and distance along the line-of-sight (LOS), the formation of hydrogen line is considered. Thus, we obtain the electron density, the neutral Hydrogen density (and consequently the ionization degree) and the emergent intensities for hydrogen lines.

PROMCOR, adapted to **gfortran** compiler, is available from MEDOC website:
https://idoc.ias.u-psud.fr/MEDOC/Radiative transfer codes

In the following sections, we will explain in details the PROMCOR code (hydrogen): modeling, implemented equations, algorithm, numerical methods, etc.

2 Description of PROMCOR code

Nature of the physical problem: Computation of the neutral H population levels in an optically thin medium. Derivation of the emission in main transition lines

Restrictions on the complexity of the problem: PROMCOR treats the hydrogen atom only

Other relevant information:
- The atmosphere model parameters considered here vary radially
- Partial frequency redistribution (PRD) is used for resonance lines of hydrogen, while for the other lines and continua complete frequency redistribution (CRD) is used

Authors: J-C. Vial and M. Chane-Yook

Program available from:
https://idoc.ias.u-psud.fr/MEDOC/Radiative transfer codes

Computer(s) on which program has been tested: PC with 4 Intel processors (2.67GHz)

Operating System(s) for which version of program has been tested: Linux

Programming language used: Adapted in Fortran 90 for **gfortran** compiler

Status: Stable

Accessibility: open (MEDOC)

No. of code lines in combined program and test deck: $\sim$ 6000

Typical running time: 6 s for one atmosphere model with about 30 points along the half LOS

Reference:
J-C. Vial and M. Chane-Yook, Neutral Hydrogen and its Emission Lines in the Solar Corona, Solar Phys., Submitted, 2016

3 Algorithm

PROMCOR and PROM5 algorithms are similar. For more details, see the documentation of PROM5.

4 Coronal modeling

Figures 1 and 2 represent respectively the image and spectra of the L_α line.

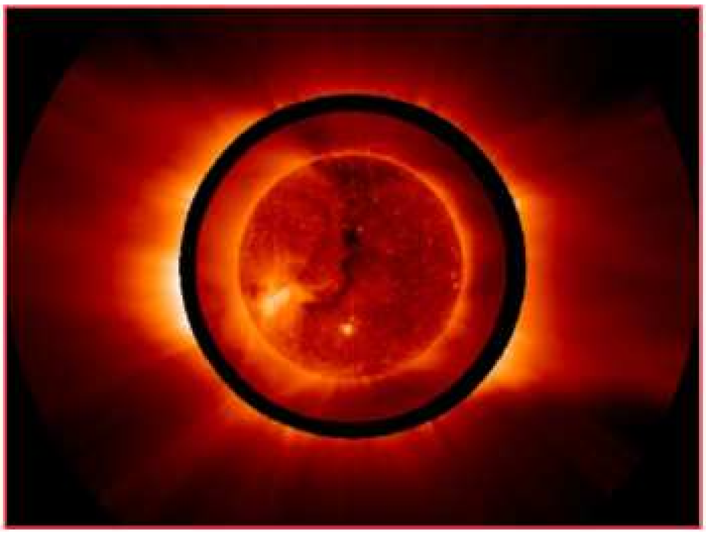

Figure 1: Observation of L_α by UVCS

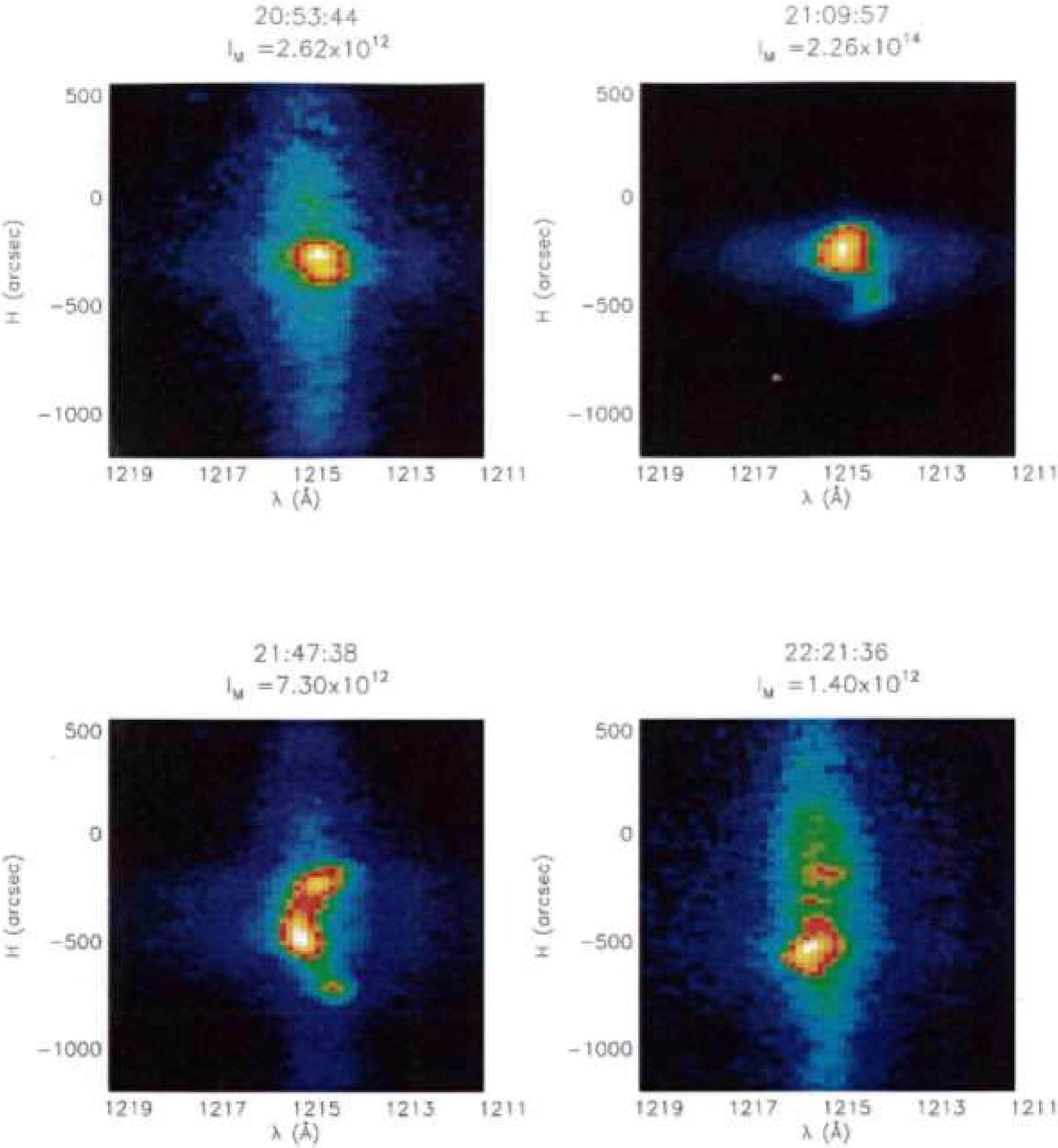

Figure 2: L_α line emission at 4 times during the observation. The initial UT time of each exposure and the line peak intensity are shown. The vertical axis is the spatial coordinate along the entrance slit, and the zero marks the 1.5 R_s heliocentric distance. Each image is scaled to its brightest pixel ([6])

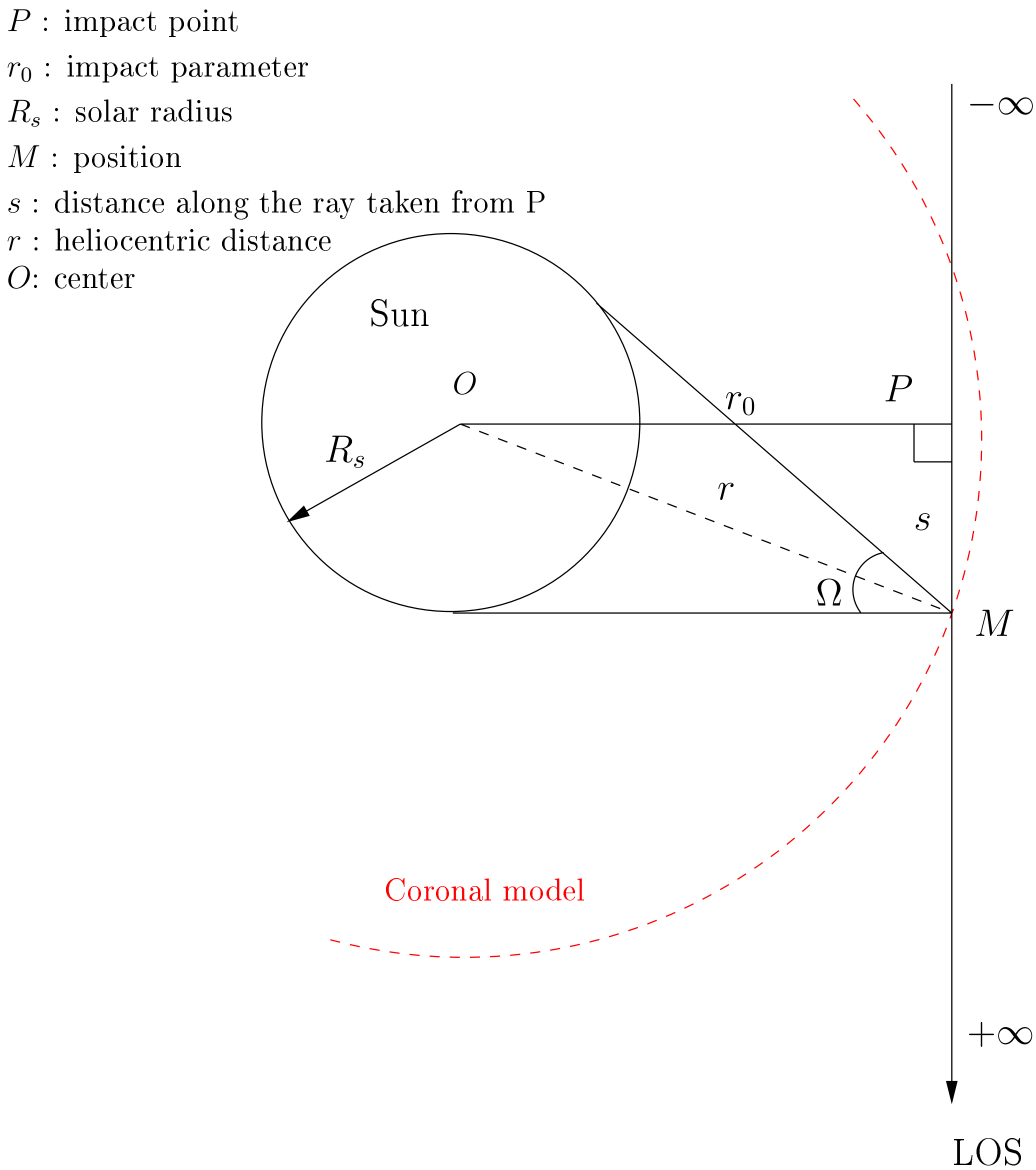

Figure 3: Coronal modelling

The initial prominence code, PROM5 is modified as follows : instead of cool core with an extended PCTR (Prominence Corona Transition region), we simply have no layer with low temperature but only a so-called PCTR with actual coronal conditions in a spherically symmetric configuration where the density (only dependent of r) decreases from the impact parameter position toward both sides of the LOS. Then, calculations can be done along the half LOS. The medium being optically thin in all lines and in all directions, the incident radiation is exactly computed at each radial distance (see Figure 3).

We adopt the same model extension, for all LOS located at altitudes between 1.05 and 5 R_s. This means that the boundaries along each LOS are (symmetrically) defined by the last external layer of the radial mode.

3 models considered in PROMCOR are described in the following sections. These models are used to produce the input model.dat file (see section 9). We select one LOS : 1.05 R_s (see section 10 for results).

4.1 Coronal hole model from Allen (1977, [1])

We adopt the radial electron density provided by Allen ([1], page 176, "pole min" values) to produce the model.dat file. We take a constant temperature of 800 000 K.

4.2 Quiet Sun model from Allen (1977, [1])

We adopt the radial electron density provided by Allen ([1], page 176, "equatorial min" values) to produce the model.dat file. We use the temperature variation with altitude of Allen([1]).

4.3 Streamer model from Goryaev ([10])

The streamer model is provided in 2D as an angular diverging slab with a Gaussian shape with a constant temperature of 1.43×10^6 K as derived from SWAP and EIS/Hinode measurements. We simplified the model into a spherically symmetric one with a constant temperature of 10^6 K. We adopt the radial electron density formula provided by Equation 16 and Table 2 from Goryaev ([10]) to produce the model.dat file.

5 Bound-Free and Bound-Bound transitions

The transitions used in PROMCOR code are Bound-Free and Bound-Bound transitions. For more details, see the documentation of PROM5.

6 Atomic structure of hydrogen

The transitions for hydrogen are summarized in Table 1. NN is the number of energy levels, including the treshold level continuum, bound levels limit (∞). $NTT = NN \times (NN - 1)/2$ is the total number of transitions, $NTAC = NN - 1$ is the number of continua (bound-free transitions) and $NTAR = NTT - NTAC$ is the number of lines (bound-bound transitions). In PROMCOR, $NN = 21$ (20 niveaux et 1 continu).

7 Population equations

For more details, see the documentation of PROM5.

Transition	Lower level	Upper level	Transition name	Wavelength $\lambda(\AA)$
1	1	2	$Ly-\alpha$	1215
2	1	3	$Ly-\beta$	1025
3	2	3	$H-\alpha$	6564
4	1	4	$Ly-\gamma$	972
5	2	4	$H-\beta$	4862
6	3	4	$Pa-\alpha$	18756
7	1	5	$Ly-\delta$	949
8	2	5	$H-\gamma$	4341
9	3	5	$Pa-\beta$	12821
10	4	5	$Br-\alpha$	6563
11	1	6	$Ly-\epsilon$	973
12	2	6	$H-\delta$	4102
13	3	6	$Pa-\gamma$	10935
14	4	6	$Br-\beta$	4861
15	5	6	$Pf-\alpha$	7460
16	1	7	$Ly-6$	931
17	2	7	$H-\epsilon$	3971
...	...	...	...	...
$NTAR+1$	1	NN	Lyman continuum	911
$NTAR+2$	2	NN	Balmer continuum	3645
...	...	...	...	...
$NTT=$	$NN-1$	NN		

Table 1: Main transitions for hydrogen

8 Formalism used for radiative transfer

The intensities are set since the medium is optically thin in all transitions. With these intensities, we compute the radiative transition rates. We start from an arbitrary electron density (half of the hydrogen density) to determine the collisional rates. Then, we solve the statistical equilibrium equations to determine hydrogen level populations and obtain new electron densities. The hydrogen densities are adjusted in order to satisfy the pressure equilibrium condition. After five iterations, we obtain hydrogen and electron densities which are consistent with the intensities.

The incident intensities are used as boundary conditions. The Lyman-α and β lines are treated according to standard partial redistribution, while complete redistribution is assumed for other lines. Since the geometry is symmetrical, computations are performed along half the LOS only. These computations produce a new set of intensities, which in turn yields new radiative rates, and new populations through the statistical equilibrium equations. In practice, "net radiative rates" (not explained here) in lines are used to control the convergence, with the help of relaxation parameters. This process is applied many times before new hydrogen and electron densities are computed to satisfy pressure and ionization equilibria.

The process stops when the convergence is reached i.e. after a total number of 40 iterations over a maximum of 400 iterations.

9 Subroutine descriptions

PROMCOR code starts by reading the input file "model.dat", by calling the main subroutine (P5EXE), by producing the output files such as line profiles given as data ("profil.dat") and by calling visualization subroutines (PSDEB, VISU21L, PSFIN). In section 9.2, each subroutine is explained in details.

Input files for PROMCOR:

- ⋆ intinc.dat : we use the same file as PROM5 to define 10 half-profiles of the chromospheric illuminating lines
- ⋆ model.dat : file including the number of integration points ($NZ = 30$), altitude of the LOS (km) and 4 columns of data. The first column corresponds to temperature T (°K), the second column to pressure P (dyn.cm^{-2}), the third column to the grid of distance along the LOS (km) and the fourth column to microturbulent velocity (km.s^{-1}). The file model.dat corresponds to either the coronal hole model (see section 4.1), or the quiet Sun model (see section 4.2) or the streamer model (see section 4.3) at a given altitude of the LOS.

Output files for PROMCOR:

- ⋆ profil.dat: line half-profiles given as data
- ⋆ profil.ps: line half-profiles as PostScript file

In the next section, hydrogen modeling will be explained in details, such as all subroutines called by PROMCOR code and a set of variables used in P5EXE subroutine.

9.1 Set of variables used in P5EXE subroutine

- IVERT=1 by default in PROMCOR
- NZ=30: number of integration points given by input file "model.dat"
- NFR=35: number of frequencies in a line

- NMU=1
- NPSOR=201: number of points for the visualization of line profiles
- NFRC=20: number of frequencies in a continuum
- NTAB=11: size of the temperature array TAB (for the computation of collision rate coefficients)
- NINF: transition lower level
- NSUP: transition upper level
- ITP: to indicate if the transition is allowed or forbidden
- IOPRN = 1: complete redistribution (CRD), IOPRN =3: partial redistribution (PRD), IOPRN = 4: PRD with coherent coefficient depending on frequency (particular case for $Ly\ \alpha$)
- IOPERA = 1: line profiles are printed, IOPERA = 0: line profiles are not printed. IOPERA is linked to DL2 (see below)
- DL1: x-axis (first wavelengths) for line profiles (visualization)
- DL2: y-axis (last wavelengths) for line profiles (visualization)
- IOPMRU = 1: only one redistribution matrix is computed for each transition (the same matrix is used for all meshs), IOPMRU = 0: all the redistribution matrices are computed for each transition (the same matrix is used for all meshs)
- EPS and BEN: line coupling coefficients
- CSI0 and ETA0: parameters for continua which are equivalent to EPS and EPSxBEN for lines
- GIBAR: mean intensity weighted by absorption profile
- IOPECO: equivalent to IOPERA for continua
- IOPFEV: option for computing variable Eddington factors
- IPROF = 1: optical depths are printed. If not, IPROF = 0
- IOPMIC = 1: microturbulent pressure is taken account. If not, IOPMIC = 0
- NVLI: number of lines to visualize
- IVHYD: visualization option for hydrogen

- INIDLD: option for initializing automatically Doppler widths from temperature of reference TEREF (for graphic representation)
- IOPCAC = 0: without continuum absorption, IOPCAC = 3: continuum absorption is included in computations
- IOPEAC: prints continuum absorption
- IOPATM: prints atmosphere parameters
- IOPTTC: prints continuum transition rates
- PMU=1: value of μ
- IVTR: visualization index for radiative transfer
- ETOT: total energy emitted by prominence for a line
- RDMAT: redistribution matrix
- AJI: Einstein A coefficient i.e. spontaneous emission
- BJI, BIJ: Einstein B coefficients for absorption and induced emission processes
- CIJ, CJI: collisional excitation/deexcitation coefficients
- CAC: continuum absorption coefficient
- TR: radiation temperature for bound-free transition
- FADIR: dilution factor for lines
- FADIC: dilution factor for continua
- CPOL: polynomial coefficients of degree 5 used in the computations of dilution factors (array size : NCMX)
- FEVK and FEVL, FKTC and FLTC : variable Eddington factors (resp. lines and continua)
- HIEMC: intensity emitted in the continuum
- RIK, RKI: radiative transition rates
- FIIR, FISR: lower and upper incident line flux
- FRR: frequency in the line

- Atmosphere parameters (array size NZ) : XM (column-mass), Z (position), TE (temperature), PG (gas pressure), VT (microturbulent velocity), HNH (hydrogen density: number of atoms per unit volume), HNE (electron density)
- NTR et NTC: discrete and bound-free transition numbers
- ICTR and ICTC: control index for lines and continua
- FRN: level frequency
- XFR and XFRC: division model in frequency for lines and continua
- BRN and BRP: net radiative bracket before and after computations (they are used to control the convergence)
- SR and SC: line and continuum source functions
- STR: total source function (for line and continuum)
- CARR: line absorption coefficient
- COHER: coherent coefficient
- OIS: collisional ionization rate coefficient

9.2 Hydrogen model (Johnson model, [16])

For more details on the Hydrogene modeling (description of the subroutines called in PROMCOR), see the documentation of PROM5.

10 Results for hydrogen lines

The half-profiles are given for an altitude of the LOS equal to 1.5 R_s, with $V_T = 5$ km.s^{-1}.

Streamer, quiet Sun and coronal models for twenty LOS are stored in the folder **results** when you download the package source file PROMCOR.tgz from the MEDOC website.

10.1 Coronal hole model from Allen (1977, [1])

E is the integrated energy in erg s^{-1} cm^{-2} sr^{-1}.

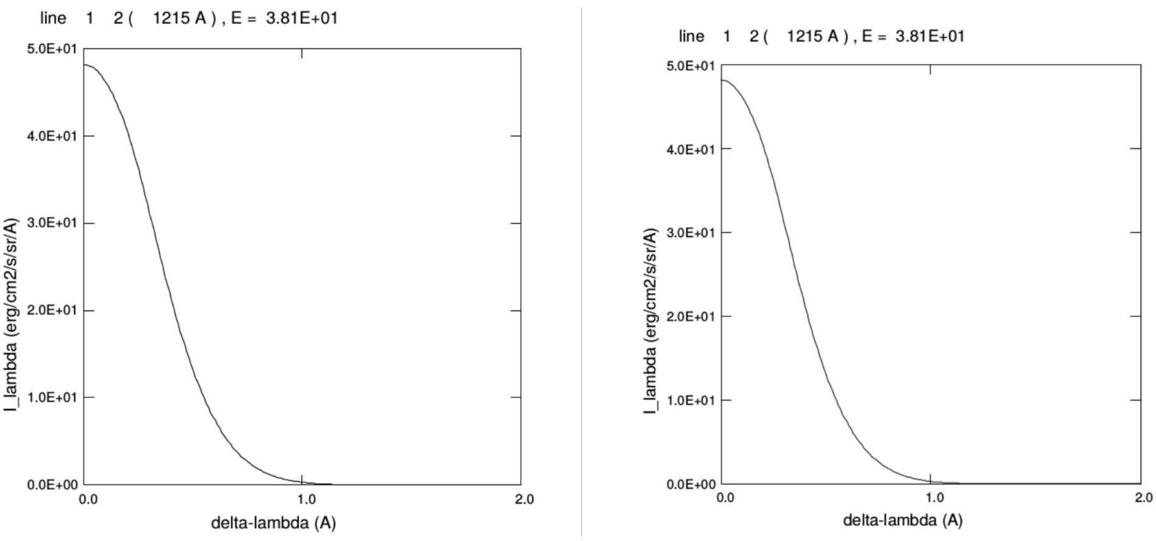

Figure 4: Half-profile of $L\alpha$ (1215 Å) line for LOS at 1.05 R_s. On the left, continuum absorption is omitted. On the right, continuum absorption is included

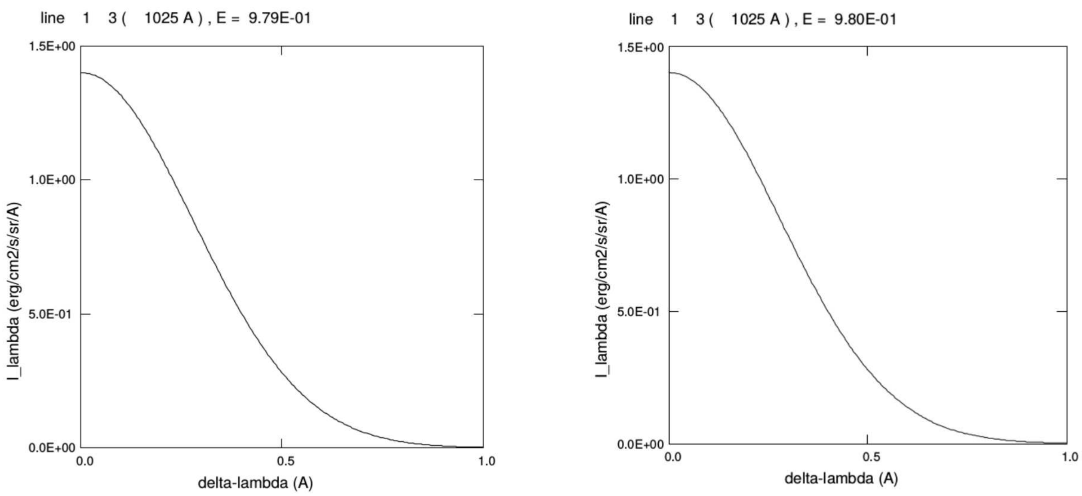

Figure 5: Half-profile of $L\beta$ (1025 Å) line for LOS at 1.05 R_s. On the left, continuum absorption is omitted. On the right, continuum absorption is included

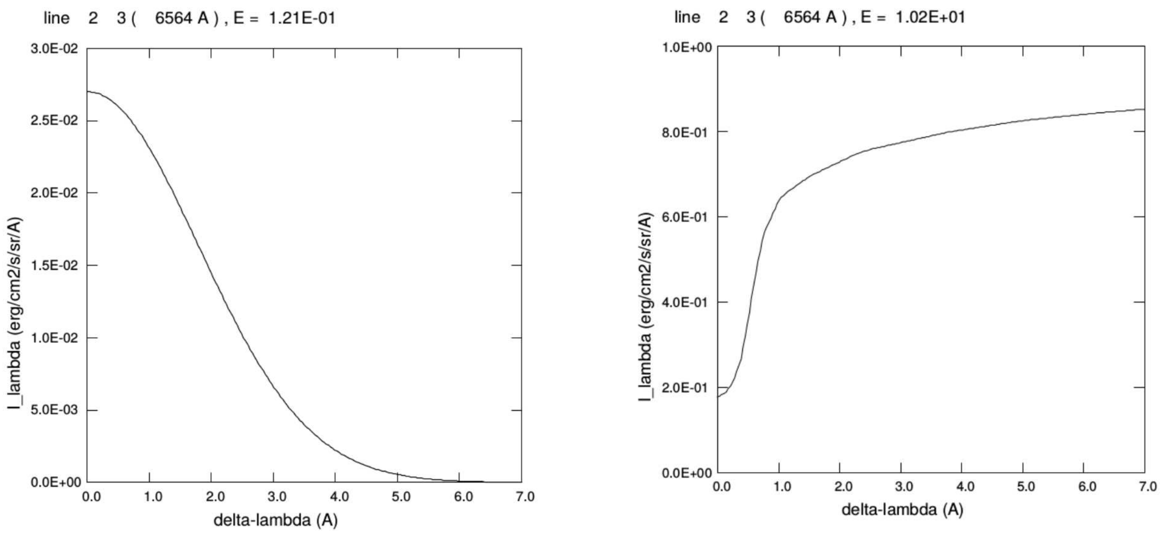

Figure 6: Half-profile of $H\alpha$ (6564 Å) line for LOS at 1.05 R_s. On the left, continuum absorption is omitted. On the right, continuum absorption is included

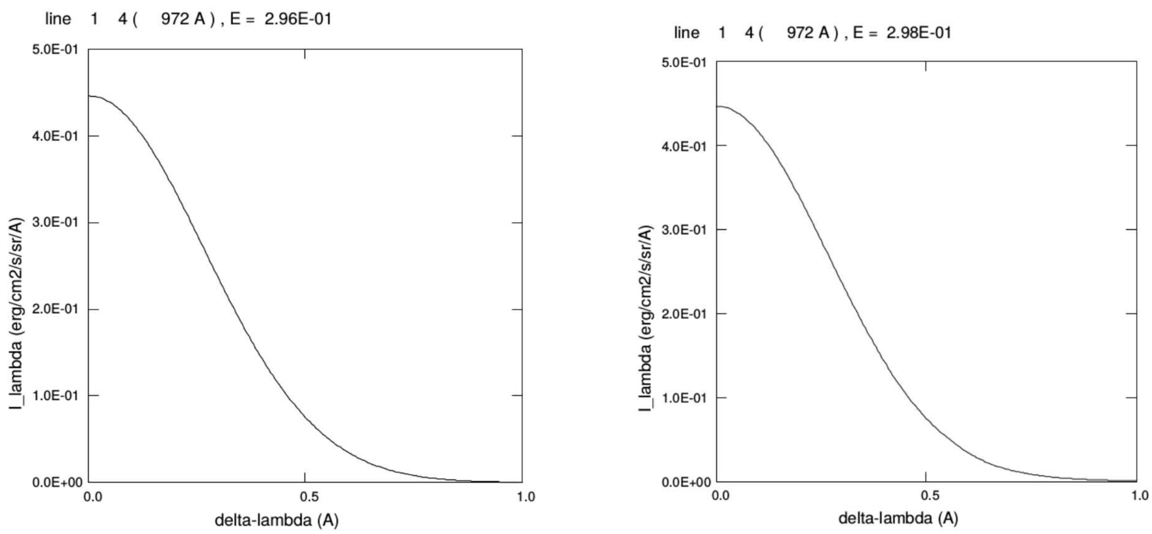

Figure 7: Half-profile of $L\gamma$ (972 Å) line for LOS at 1.05 R_s. On the left, continuum absorption is omitted. On the right, continuum absorption is included

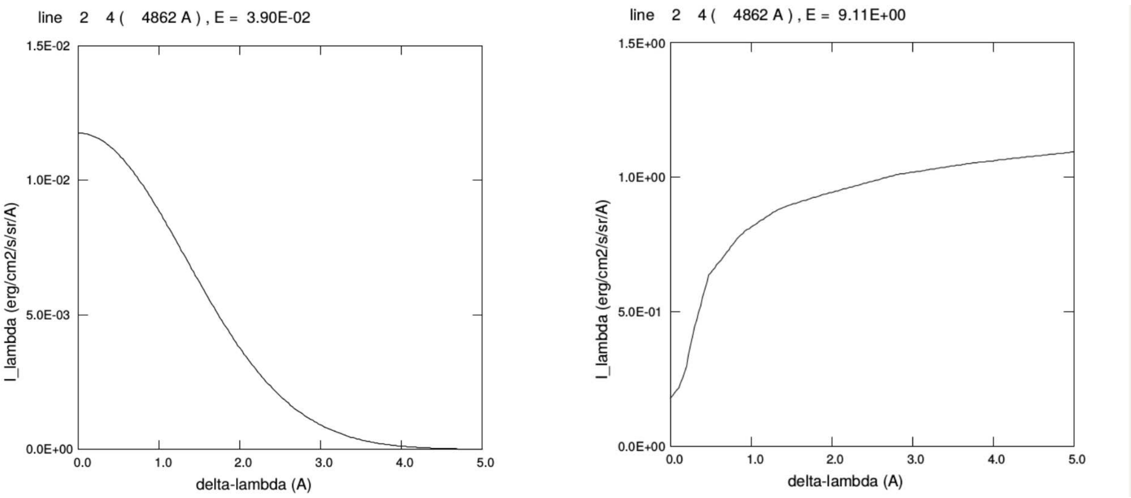

Figure 8: Half-profile of $H\beta$ (4862 Å) line for LOS at 1.05 R_s. On the left, continuum absorption is omitted. On the right, continuum absorption is included

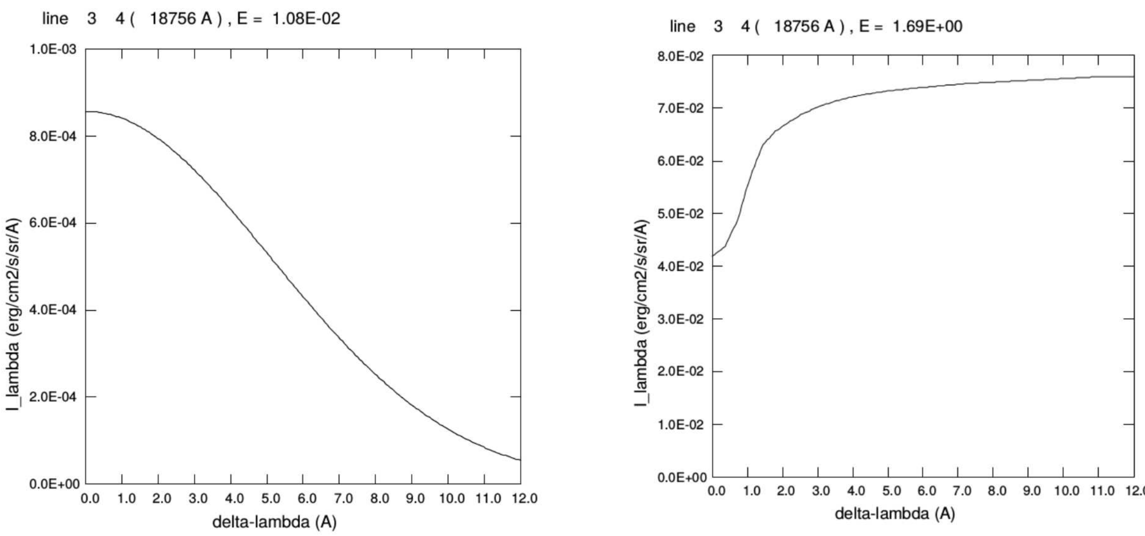

Figure 9: Half-profile of $Pa-\alpha$ (18756 Å) line for LOS at 1.05 R_s. On the left, continuum absorption is omitted. On the right, continuum absorption is included

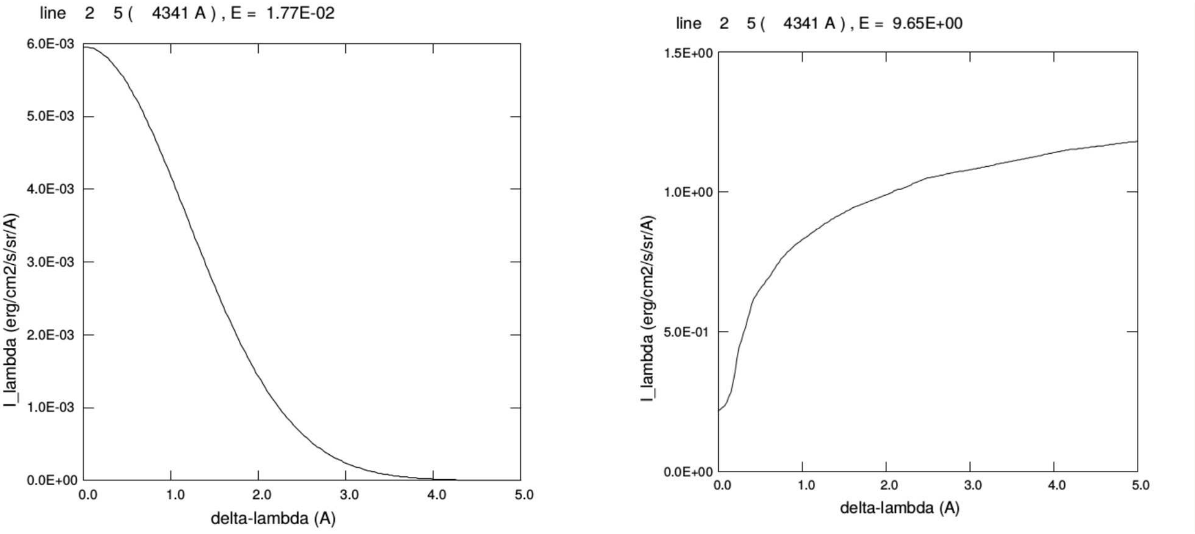

Figure 10: Half-profile of $H\gamma$ (4341 Å) line for LOS at 1.05 R_s. On the left, continuum absorption is omitted. On the right, continuum absorption is included

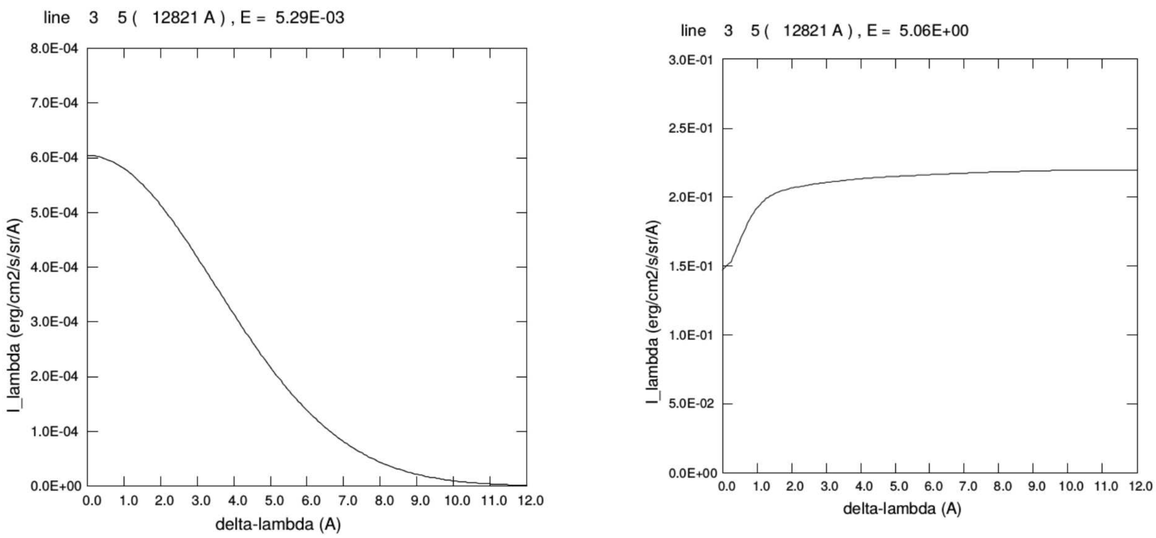

Figure 11: Half-profile of $Pa-\beta$ (12821 Å) line for LOS at 1.05 R_s. On the left, continuum absorption is omitted. On the right, continuum absorption is included

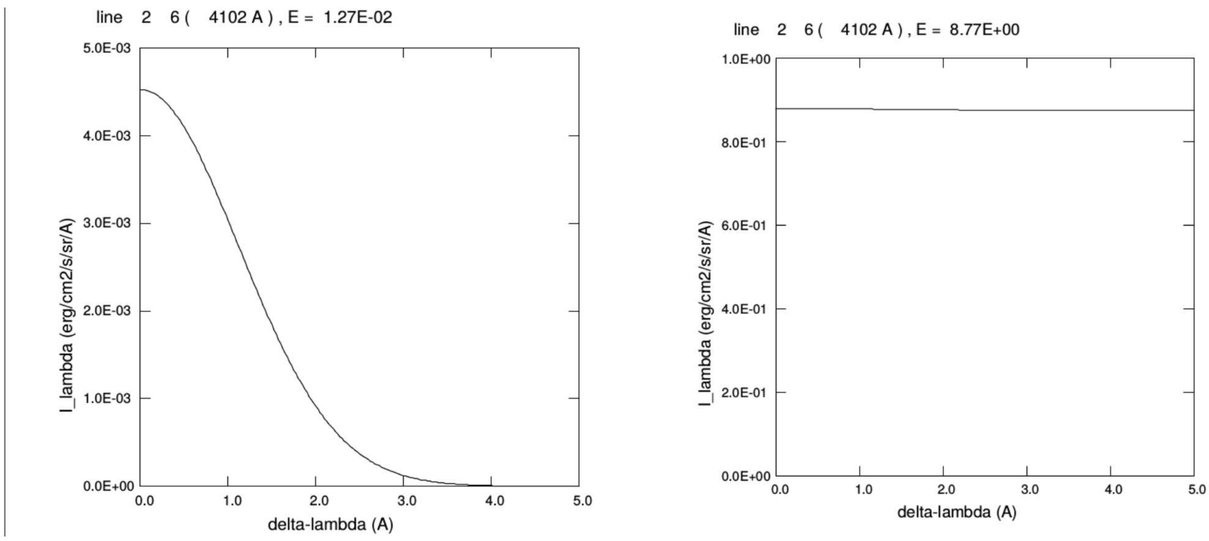

Figure 12: Half-profile of $H\delta$ line (4102 Å) for LOS at 1.05 R_s. On the left, continuum absorption is omitted. On the right, continuum absorption is included

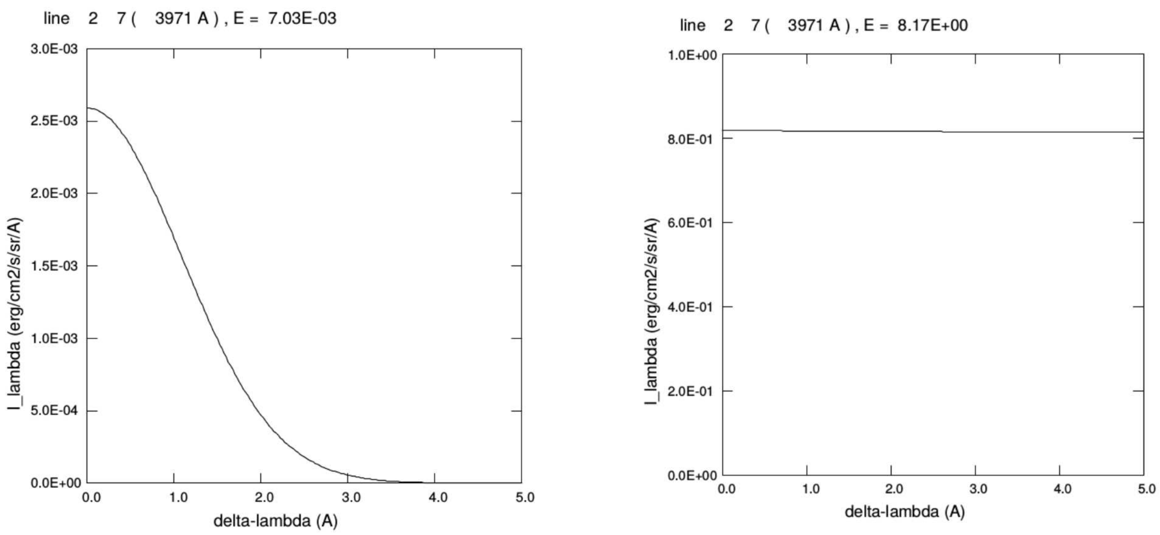

Figure 13: Half-profile of $H\epsilon$ line (3971 Å) for LOS at 1.05 R_s. On the left, continuum absorption is omitted. On the right, continuum absorption is included

10.2 Quiet Sun model from Allen (1977, [1])

E is the integrated energy in erg s^{-1} cm^{-2} sr^{-1}.

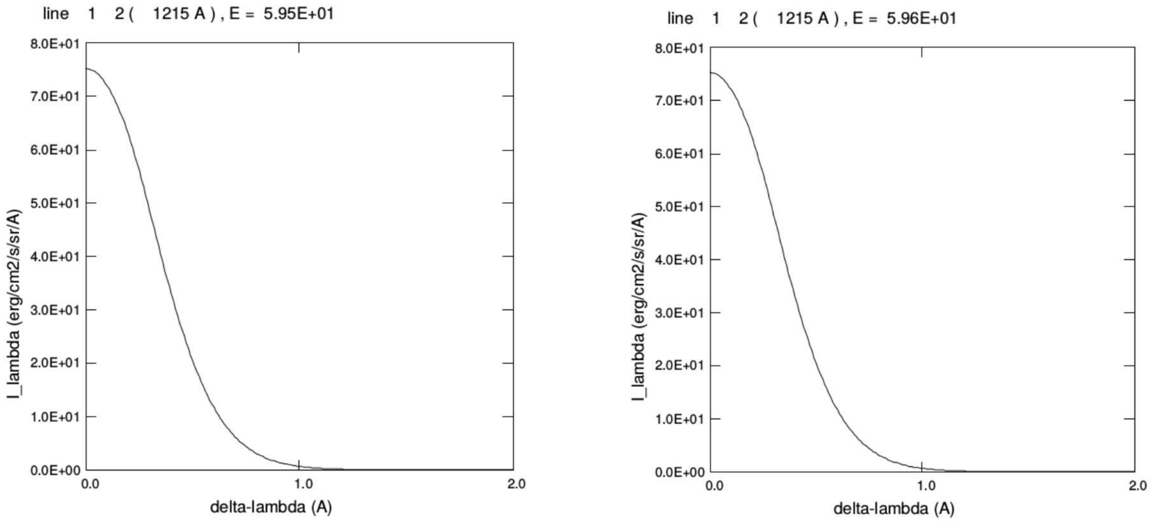

Figure 14: Half-profile of $L\alpha$ (1215 Å) line for LOS at 1.05 R_s. On the left, continuum absorption is omitted. On the right, continuum absorption is included

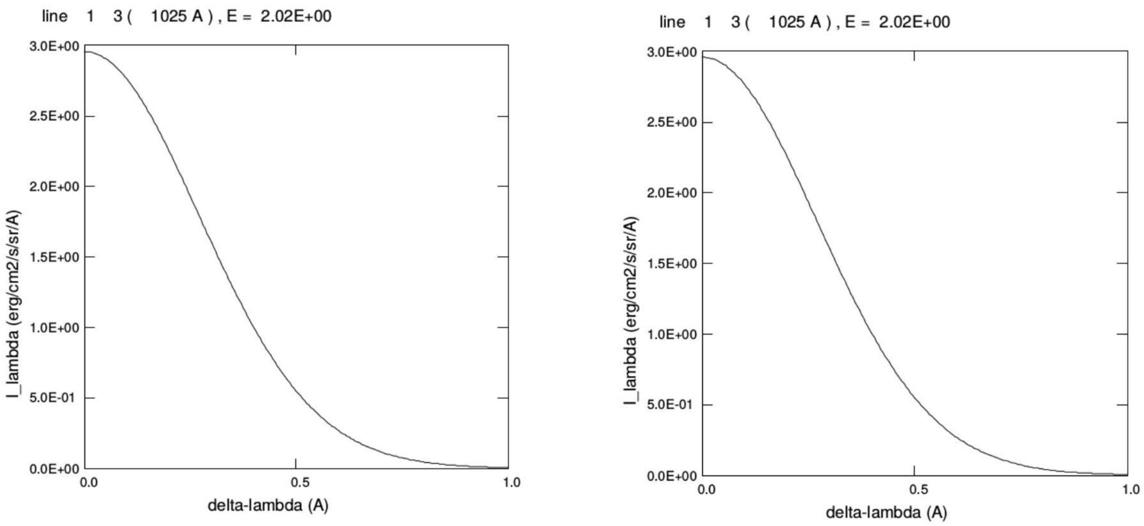

Figure 15: Half-profile of $L\beta$ (1025 Å) line for LOS at 1.05 R_s. On the left, continuum absorption is omitted. On the right, continuum absorption is included

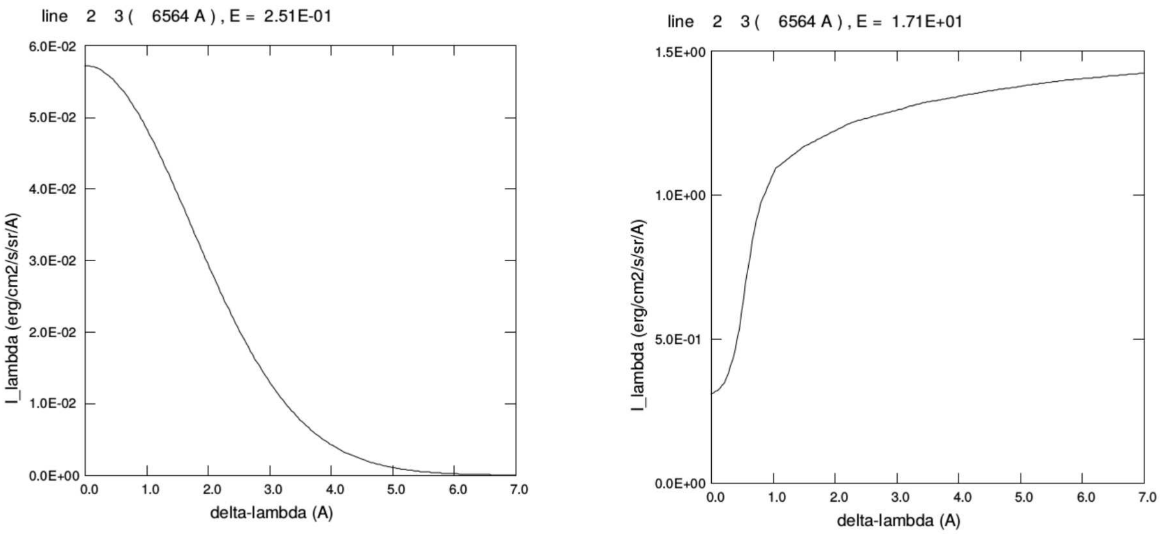

Figure 16: Half-profile of $H\alpha$ (6564 Å) line for LOS at 1.05 R_s. On the left, continuum absorption is omitted. On the right, continuum absorption is included

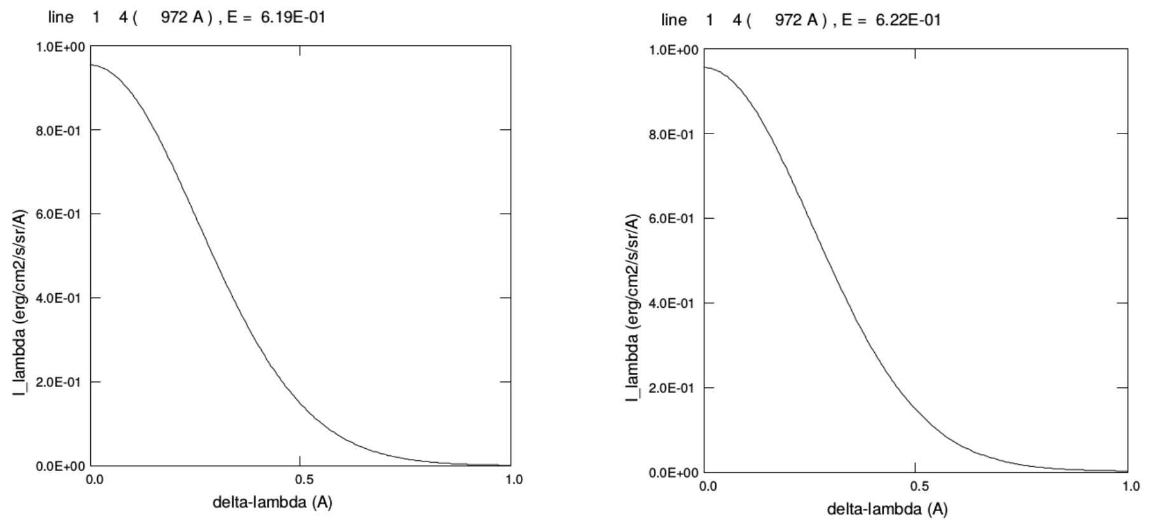

Figure 17: Half-profile of $L\gamma$ (972 Å) line for LOS at 1.05 R_s. On the left, continuum absorption is omitted. On the right, continuum absorption is included

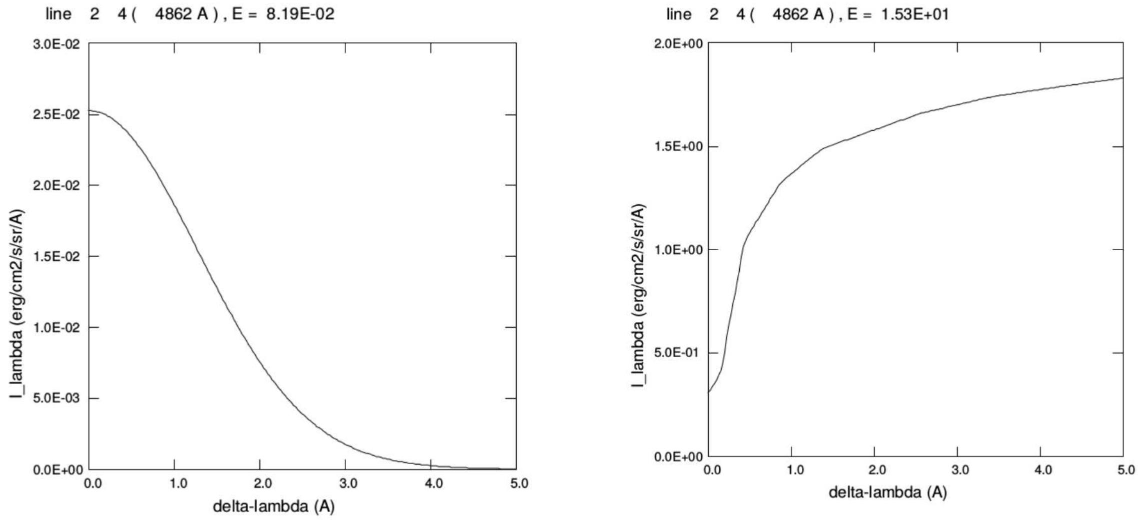

Figure 18: Half-profile of $H\beta$ (4862 Å) line for LOS at 1.05 R_s. On the left, continuum absorption is omitted. On the right, continuum absorption is included

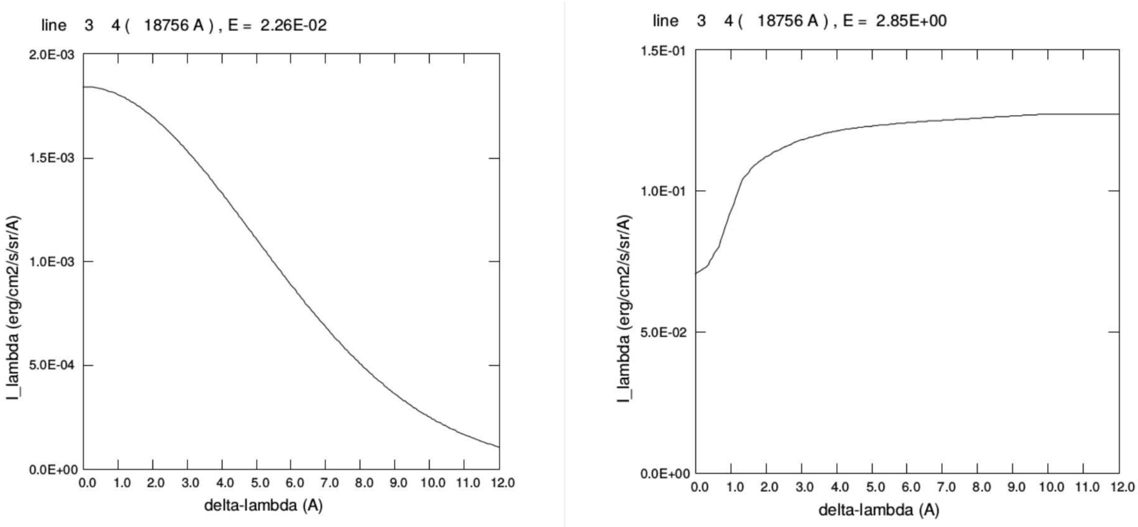

Figure 19: Half-profile of $Pa - \alpha$ (18756 Å) line for LOS at 1.05 R_s. On the left, continuum absorption is omitted. On the right, continuum absorption is included

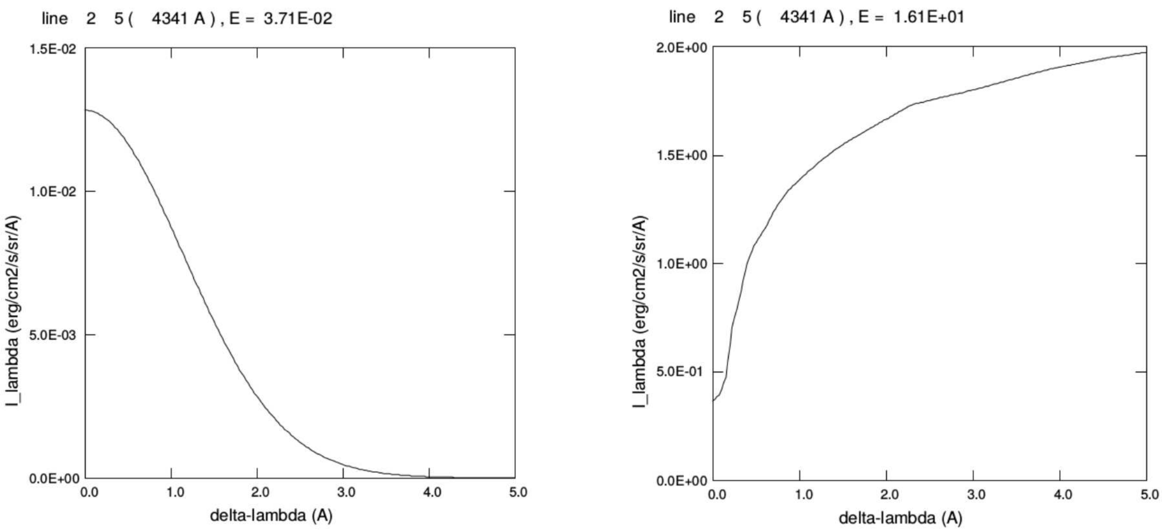

Figure 20: Half-profile of $H\gamma$ (4341 Å) line for LOS at 1.05 R_s. On the left, continuum absorption is omitted. On the right, continuum absorption is included

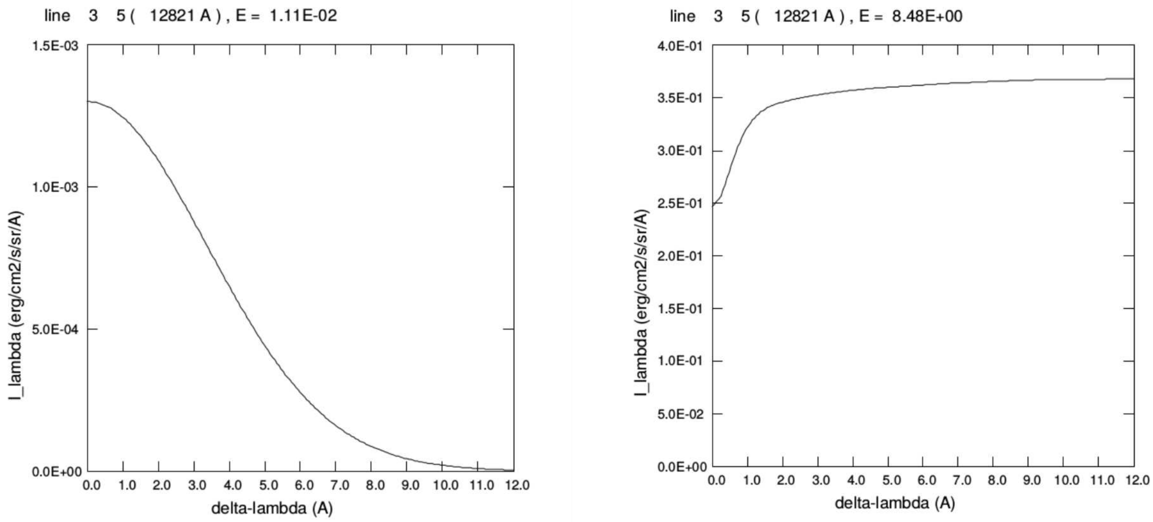

Figure 21: Half-profile of $Pa-\beta$ (12821 Å) line for LOS at 1.05 R_s. On the left, continuum absorption is omitted. On the right, continuum absorption is included

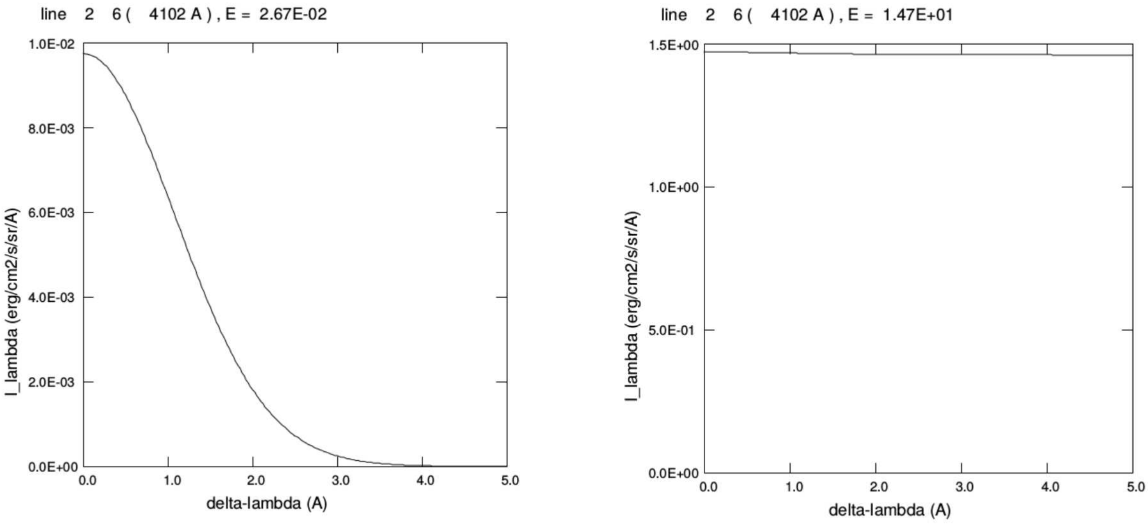

Figure 22: Half-profile of $H\delta$ line (4102 Å) for LOS at 1.05 R_s. On the left, continuum absorption is omitted. On the right, continuum absorption is included

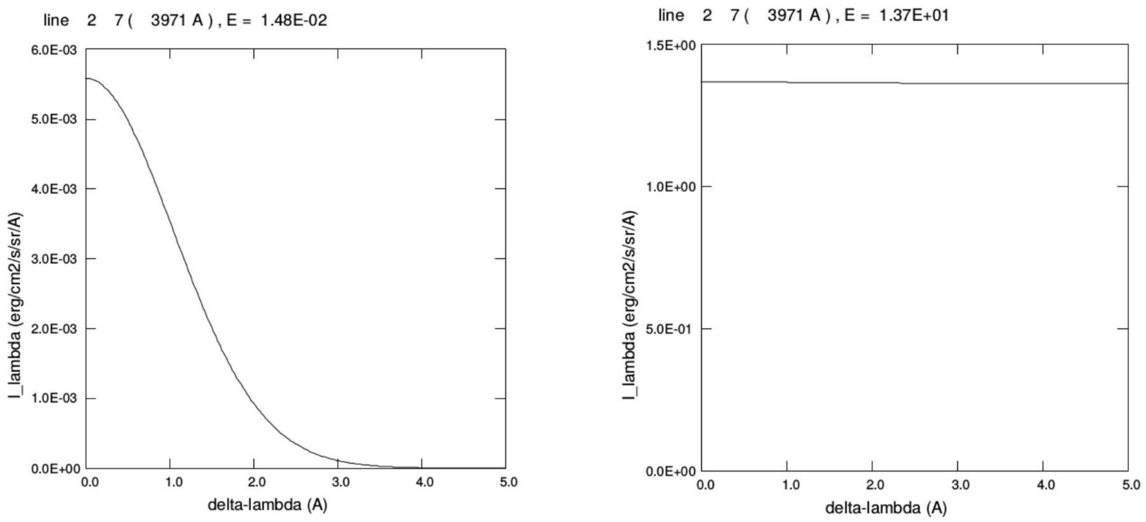

Figure 23: Half-profile of $H\epsilon$ line (3971 Å) for LOS at 1.05 R_s. On the left, continuum absorption is omitted. On the right, continuum absorption is included

10.3 Streamer model from Goryaev ([10])

E is the integrated energy in erg s^{-1} cm^{-2} sr^{-1}.

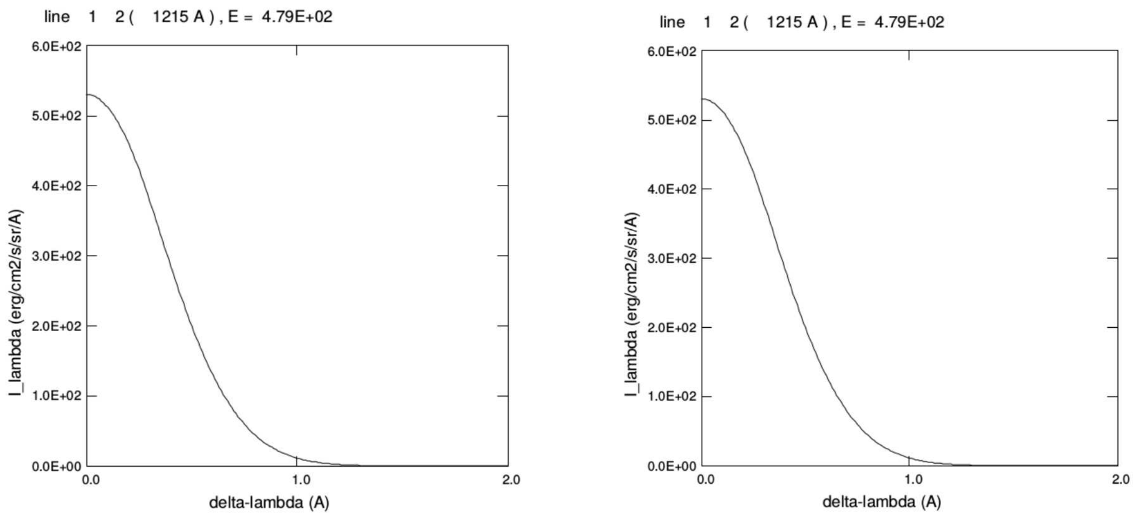

Figure 24: Half-profile of $L\alpha$ (1215 Å) line for LOS at 1.05 R_s. On the left, continuum absorption is omitted. On the right, continuum absorption is included

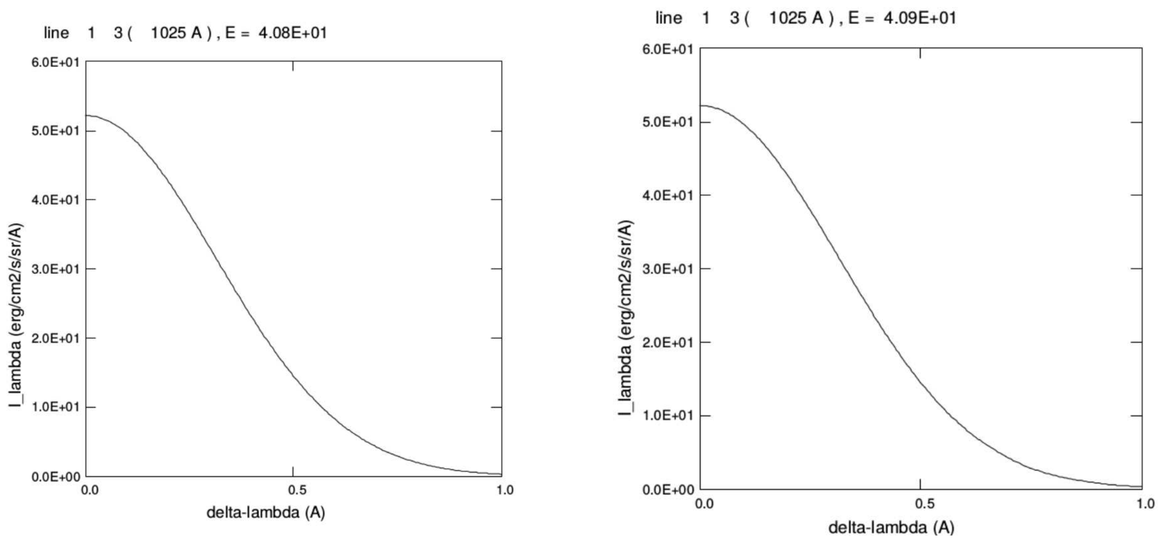

Figure 25: Half-profile of $L\beta$ (1025 Å) line for LOS at 1.05 R_s. On the left, continuum absorption is omitted. On the right, continuum absorption is included

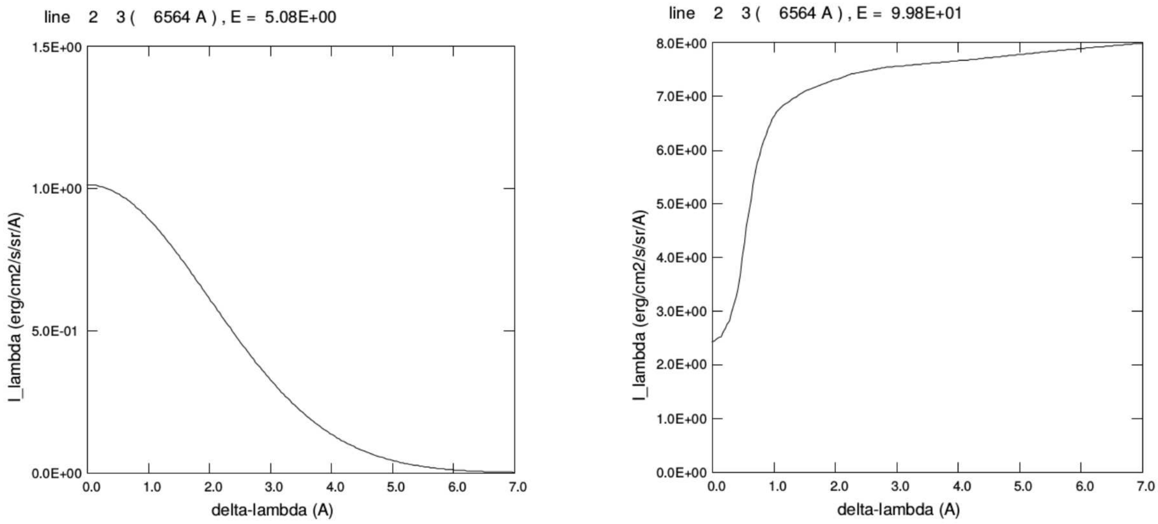

Figure 26: Half-profile of $H\alpha$ (6564 Å) line for LOS at 1.05 R_s. On the left, continuum absorption is omitted. On the right, continuum absorption is included

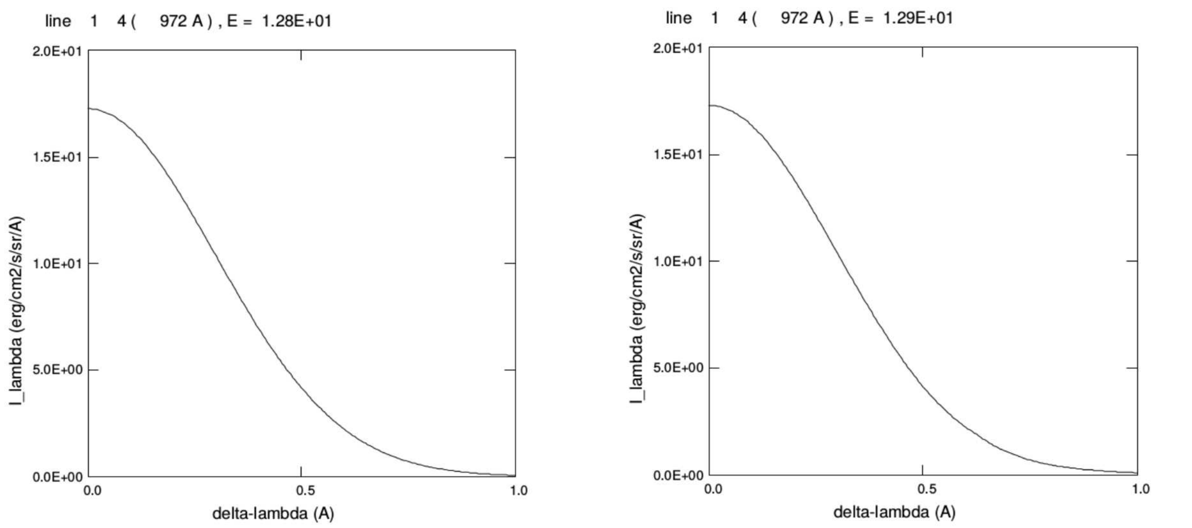

Figure 27: Half-profile of $L\gamma$ (972 Å) line for LOS at 1.05 R_s. On the left, continuum absorption is omitted. On the right, continuum absorption is included

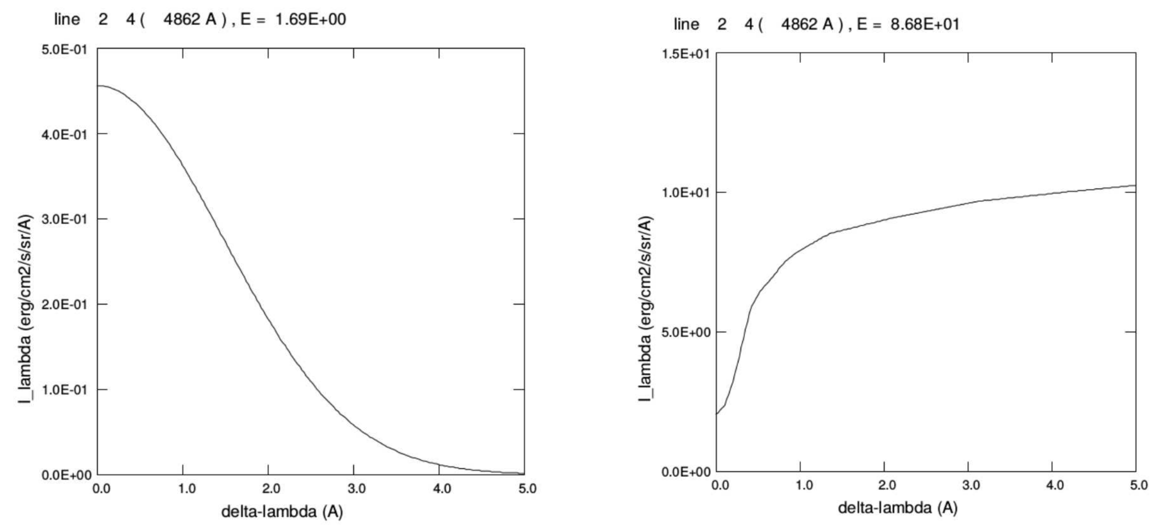

Figure 28: Half-profile of $H\beta$ (4862 Å) line for LOS at 1.05 R_s. On the left, continuum absorption is omitted. On the right, continuum absorption is included

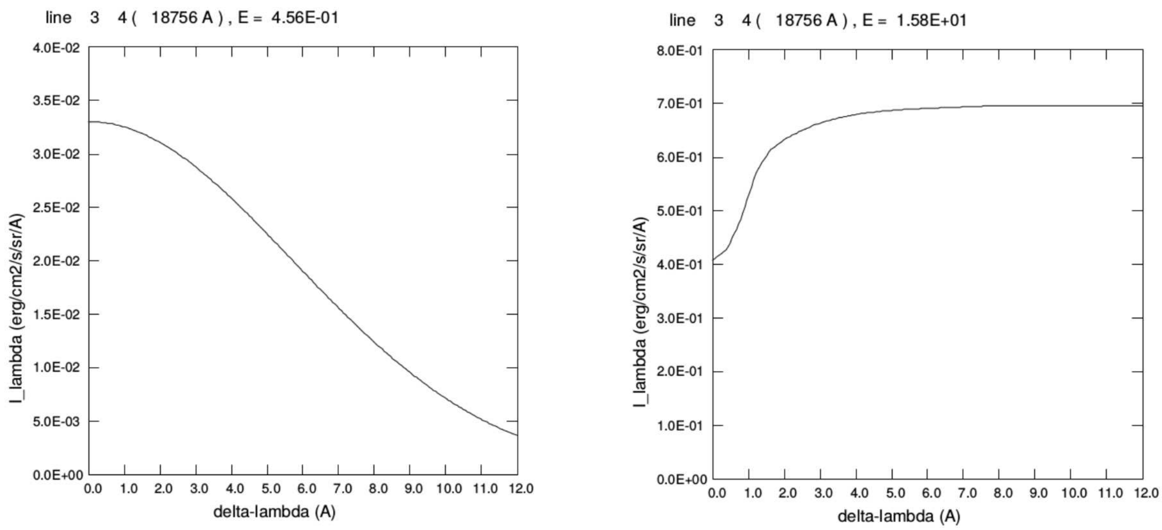

Figure 29: Half-profile of $Pa-\alpha$ (18756 Å) line for LOS at 1.05 R_s. On the left, continuum absorption is omitted. On the right, continuum absorption is included

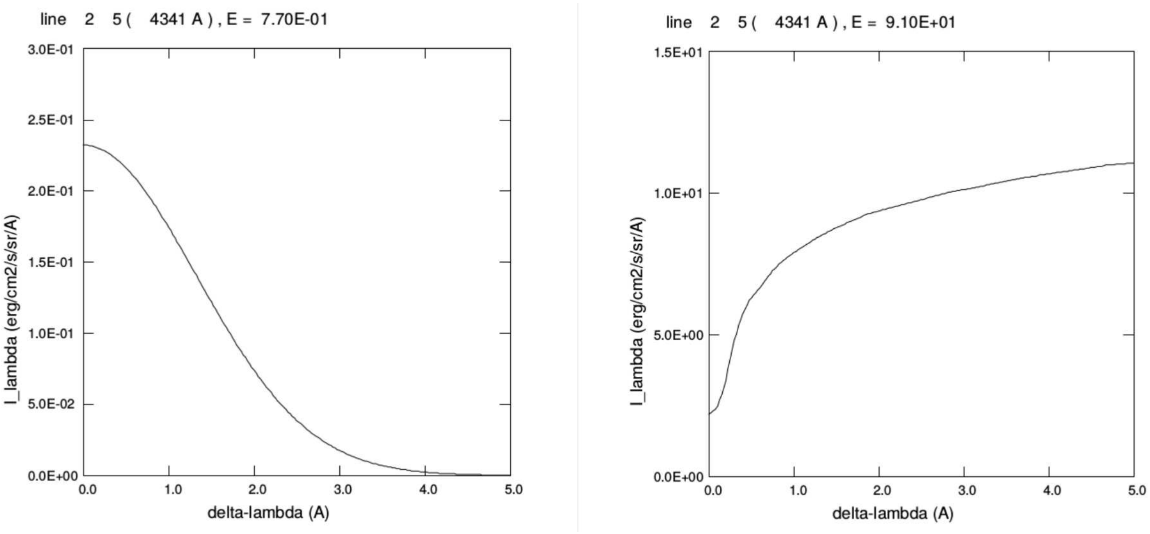

Figure 30: Half-profile of $H\gamma$ (4341 Å) line for LOS at 1.05 R_s. On the left, continuum absorption is omitted. On the right, continuum absorption is included

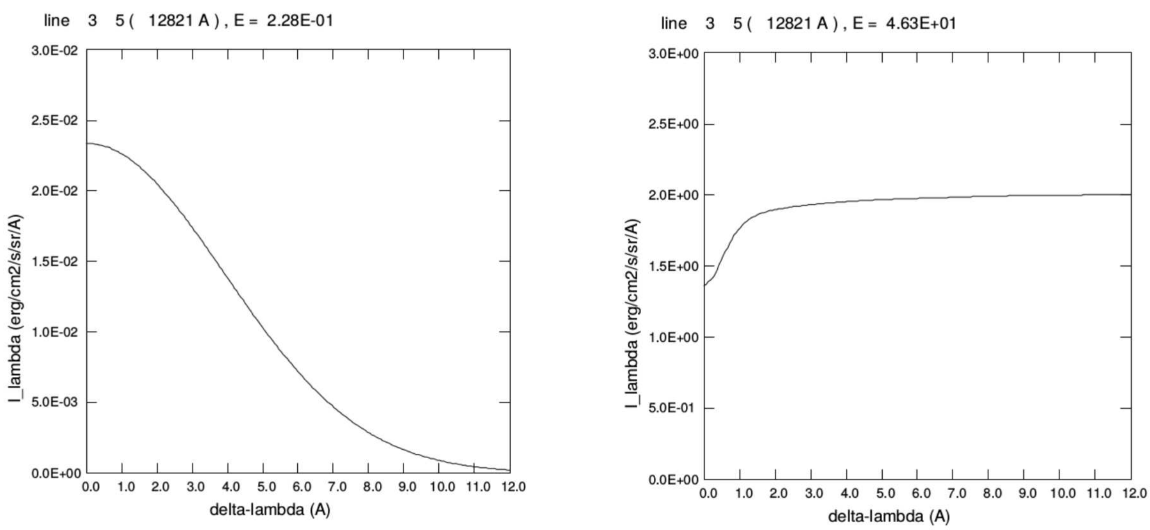

Figure 31: Half-profile of $Pa-\beta$ (12821 Å) line for LOS at 1.05 R_s. On the left, continuum absorption is omitted. On the right, continuum absorption is included

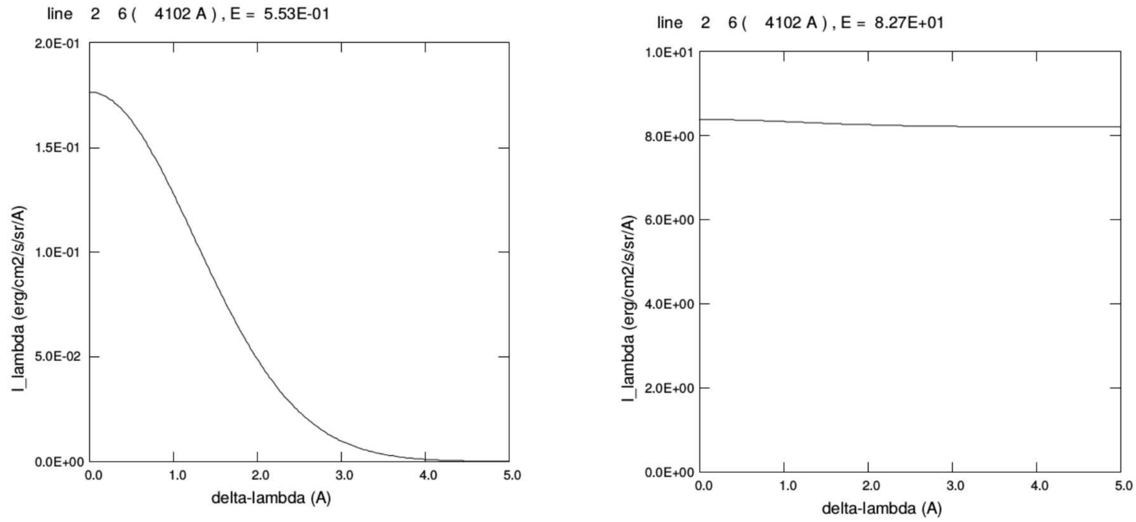

Figure 32: Half-profile of $H\delta$ line (4102 Å) for LOS at 1.05 R_s. On the left, continuum absorption is omitted. On the right, continuum absorption is included

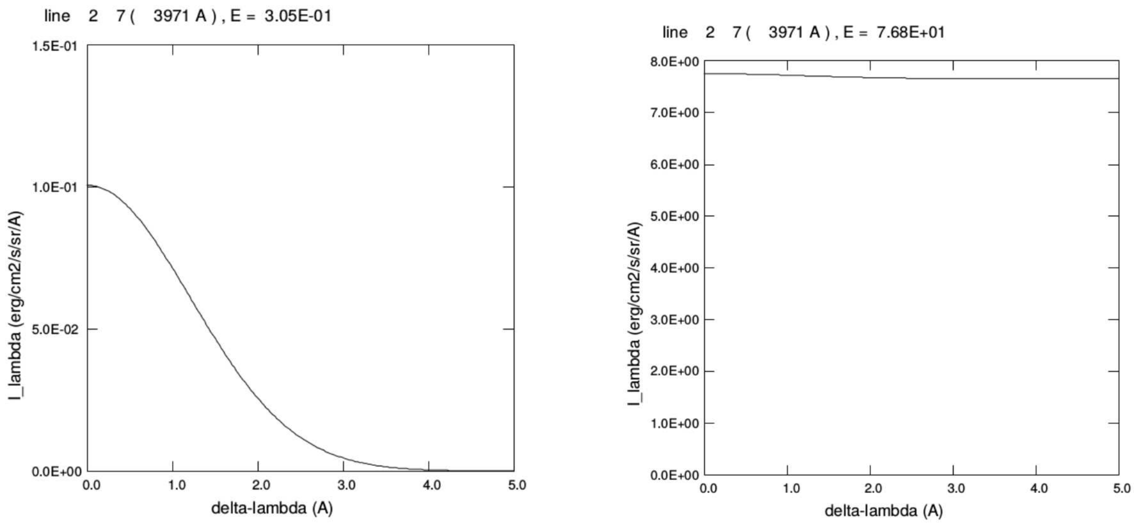

Figure 33: Half-profile of $H\epsilon$ line (3971 Å) for LOS at 1.05 R_s. On the left, continuum absorption is omitted. On the right, continuum absorption is included

11 Running PROMCOR

- Download the package PROMCOR.tgz from MEDOC website: https://idoc.ias.u-psud.fr/MEDOC/Radiative transfer codes/PROMCOR
- gfortran compiler is required.

- Unpack the package by typing the following linux command:
  tar -xvzf PROMCOR.tgz
- Go to folder PROMCOR:
  cd PROMCOR
- The folder contains the following files: intinc.dat, model.dat, makefile, promcor.f90
- Run the code by typing:
  make
  ./promcor
- The ouput files are: profil.dat, profil.ps
- The folder **results** contains the output files corresponding to a test case to be able to check if your results are good.

12 CPU time

On a PC with 4 Intel processors (2.67 GHz), the CPU time for PROMCOR code with the coronal hole model ("model.dat") is: 6 s.

13 Acknowledgements

We thank MEDOC director Eric Buchlin for his support.

17th June 2016
M. C-Y

References

[1] C.W. Allen. *Astrophysical quantities.* The Athlone Press, University of London, 1973.

[2] M. Arnaud and R. Rothenflug. An updated evaluation of recombination and ionization rates. *A&A suppl. Ser.*, 60:425–457, 1985.

[3] L.H. Auer and D. Mihalas. On the use of variable Eddington factors in Non-LTE stellar atmospheres computations. *Mon. Not. R. astr. Soc*, 149:65–74, 1970.

[4] Eugene H. Avrett. *Introduction to Non-LTE radiative transfer and atmospheric modeling.* Lecture notes, 2008.

[5] S. Chandrasekhar. *Radiative transfer.* Dover Publications, 1960.

[6] A. Ciaravella, J. C. Raymond, S. Fineschi, M. Romoli, C. Benna, L. Gardner, S. Giordano, J. Michels, R. O'Neal, E. Antonucci, J. Kohl, and G. Noci. Ultraviolet Coronagraph Spectrometer Observation of the 1996 December 23 Coronal Mass Ejection. , 491:L59–L62, December 1997.

[7] CHIANTI Database. George Mason University (USA) and University of Michigan (USA) and University of Cambridge (UK). *http://www.chiantidatabase.org/*, Mai 2014.

[8] K.P. Dere, E. Landi, H.E. Mason, B.C. Monsignori Fossi, and P.R. Young. CHIANTI - an atomic database for emission lines: I. Wavelengths greater than 50a. *A&A suppl. Ser.*, 125:149–173, 1997.

[9] O. Gingerich. Review of Opacity Calculations. *Proceedings of the First Harvard-Smithsonian Conference on Stellar Atmospheres*, 167:1–25, 1964.

[10] F. Goryaev, V. Slemzin, L. Vainshtein, and D. R. Williams. Study of Extreme-ultraviolet Emission and Properties of a Coronal Streamer from PROBA2/SWAP, Hinode/EIS and Mauna Loa Mk4 Observations. , 781:100, February 2014.

[11] P. Gouttebroze, P. Heinzel, and J.-C. Vial. The hydrogen spectrum of model prominences. *A&A Suppl. Ser.*, 99:513–543, 1993.

[12] P. Gouttebroze and N. Labrosse. A ready-made code for the computation of prominence NLTE medels. *Solar Physics*, 196:349–355, 2000.

[13] Pierre Gouttebroze. *Formation des raies spectrales et oscillations dans la chromosphère solaire.* Thèse d'Etat, Université Paris 7, 1980.

[14] I. Hubeny and D. Mihalas. *Theory of Stellar Atmospheres : An introduction to Astrophysical Non-equilibrium Quantitative Spectroscopic Analysis.* Princeton University Press, 2015.

[15] J.T. Jefferies. *Spectral line formation.* Blaisdell, 1968.

[16] L.C. Johnson. Approximation for collisional and radiative transition rates in atomic hydrogen. *A&A*, 174:227–236, 1972.

[17] Nicolas Labrosse. *Modélisation du spectre de l'hélium dans les protubérances solaires.* PhD thesis, Université Paris XI Orsay, 2001.

[18] P. Lemaire, P. Gouttebroze, J.-C. Vial, and G. E. Artzner. Physical properties of the solar chromosphere deduced from optically thick lines: I. Observations, data reduction, and modelling of an average plage. *A&A*, 103:160–176, 1981.

[19] J. Oxenius. *Kinetic Theory of Particles and Photons. Theoretical Foundations of Non-LTE Plasma Spectroscopy.* Springer-Verlag, 1986.

[20] G. Peach. A general formula for the calculation of absorption cross sections for free-free trabsitions in the field of positive ions. *Royal Astronomical Society*, 130:361–377, 1964.

[21] C. Pecker-Wimel. *Introduction à la spectroscopie des plasmas.* Gordon and Breach, 1966.

[22] R.J. Rutten. *Radiative transfer in stellar atmospheres.* 2003.

[23] E. Schatzman. *Astrophysique.* Masson et Cie, 1963.

[24] J.E. Vernazza, E. H. Avrett, and R. Loeser. Structure of the Solar chromosphere; ii. The underlying photosphere and temperature-minimum region. *ApJS*, 30:1–60, 1976.

[25] J-C. Vial and M. Chane-Yook. Neutral Hydrogen and its Emission Lines in the Solar Corona. *Solar Phys.*, Submitted, 2016.